

# Determination of the Depth of Cut via Surface Integrity

Cristina Gavrus<sup>1</sup>, Nicolae-Valentin Ivan<sup>2</sup> and Gheorghe Oancea<sup>2,\*</sup> 

<sup>1</sup> Department of Engineering and Industrial Management, Transilvania University of Brasov, B-dul Eroilor 29, 500036 Brasov, Romania; cristina.gavrus@unitbv.ro

<sup>2</sup> Department of Manufacturing Engineering, Transilvania University of Brasov, B-dul Eroilor 29, 500036 Brasov, Romania; nivivan@unitbv.ro

\* Correspondence: gh.oancea@unitbv.ro

**Abstract:** The present paper continues the authors' research in machining process optimization, including the direction of machining parameters optimization. The paper develops an innovative method, via surface integrity, for determining the technological route and the related depths of cut, with respect to machining front faces of cast iron parts. For correctly establishing the depths of the cut, the errors that appear within surface and subsurface layers during the casting process, as well as during machining, must be gradually eliminated. These errors make it necessary to consider the concept of surface integrity. This paper presents the modality of integrating the components of surface integrity into the depth of cut. For the practical use of this method, a new software tool based on a series of mathematical models and a small database was conceived. A case study illustrates how the method is applied and the software tool used to solve a specific application in the case of a belt pulley.

**Keywords:** surface integrity; facing turning; sequence of operations; depth of cut; cast iron parts; software tool



**Citation:** Gavrus, C.; Ivan, N.-V.; Oancea, G. Determination of the Depth of Cut via Surface Integrity. *Appl. Sci.* **2023**, *13*, 6881. <https://doi.org/10.3390/app13126881>

Academic Editor: Abílio Manuel Pinho de Jesus

Received: 25 April 2023

Revised: 31 May 2023

Accepted: 5 June 2023

Published: 6 June 2023



**Copyright:** © 2023 by the authors. Licensee MDPI, Basel, Switzerland. This article is an open access article distributed under the terms and conditions of the Creative Commons Attribution (CC BY) license (<https://creativecommons.org/licenses/by/4.0/>).

## 1. Introduction and Literature Review

An important part of process planning refers to establishing the machining parameters. The depth of cut is the parameter that directly influences the machined-surface quality because it interacts with both the surface and subsurface layers of the processed material. The machined-surface quality must not be appreciated only by the surface roughness. A correct assessment must consider the condition and characteristics of the surface, as well as of the subsurface of the processed material. Thus, surface integrity becomes a very important criterion for assessing the quality of the machined surface [1,2]. Surface integrity refers to certain aspects of the surface, such as form, roughness, waviness, lay, and subsurface characteristics such as residual stress, granular plastic flow orientation, and defects (porosity, micro cracks, tears, laps, etc.) [3]. Surface integrity is influenced by various factors, including the machining parameters [4–6]. Dumas et al. [7] approach the connection between the rough and finishing tool passes considering the final surface integrity. The final surface integrity is influenced by the previous operations/passes. Surface integrity is specific to each operation. Thus, the concept of Current-Previous Machining Process—CPMP [8] becomes very important. This concept considers that surface roughness  $Rz_p$  and the components of  $S_p$  generated during the machining process and caused by the casting process must be considered when calculating  $d_{cf}$  (current depth of cut), following Figure 1.  $Rz_p$  refers to the surface roughness obtained after the previous operation.  $S_p$  refers to the subsurface layer degraded after the previous operation (subsurface defects). The depth of cut must also contain dimensional tolerance obtained at the previous operation ( $\delta_p$ ), flatness deviation obtained after the previous operation ( $\epsilon F_p$ ), and axial clamping error related to the current operation ( $\epsilon Cax_c$ ). Among the first researchers who have considered the connection between the depth of cut and machined-surface quality was

Kovan [9,10], whose ideas were overtaken by Picos [11], as well. However, at that time, the term surface integrity was not known. This term was first used by M. Field, J. F. Kahles in 1964. In accordance with these papers, the components of  $d_{cf}$  are colinear vectors, as Formula (1) illustrates.

$$d_{cf} \geq Rz_p + S_p + \delta_p + \epsilon F_p + \epsilon C a x_c \tag{1}$$

index  $p$  is used for the previous operation, and index  $c$  is used for the current operation, so  $d_{cf}$  is to be calculated. In the literature, establishing the depth of cut is approached with respect to the issue of cutting parameters optimization. The depth of cut, as well as the other machining parameters, results based on a mathematical optimization model. Usually, the optimization criterion is an economic one (minimization of cost and time regarding machining operations). The constraints from the mathematical models are connection relations among the parameters related to machining operations. Pratihari [12] overviews the software for modeling certain parameters related to machining operations. The paper considers expert systems. Regarding the turning processes, the considered parameters are feed, depth of cut, speed, and surface roughness. Zhu et al. [13] present connection relations among surface roughness, work piece speed, tool speed, depth of cut, and feed. Baburaj et al. [14] created relations among surface roughness, cutting speed, feed rate, depth of cut, and nose radius. Prasad and Babu [15] have studied how vibration amplitude and tool flank wear were influenced by machining parameters. Table 1 presents an overview of optimization methods used by certain authors.

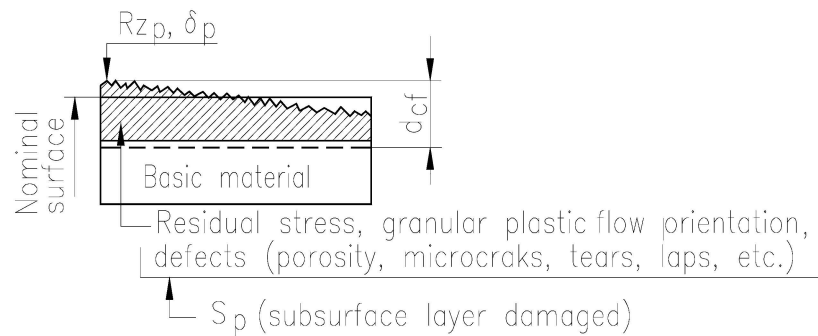


Figure 1. Components of the surface integrity.

Table 1. Optimization techniques for machining parameters.

Paper	Optimization Mathematical Methods	
	Traditional	Non-Traditional
[16]	Dynamic programming	
[17]		Neural network
[18]	Integer programming	
[19]		Simulated annealing, Hooke–Jeeves pattern search
[20]		Genetic algorithm
[21]		Scatter search
[22]		Genetic algorithm
[23]		Genetic algorithm
[24]		genetic algorithm, simulated annealing, ant colony optimization
[25]		Evolutionary strategy
[26]		Particle swarm optimization

Table 1. Cont.

Paper	Optimization Mathematical Methods	
	Traditional	Non-Traditional
[27]		Simulated annealing, genetic algorithm, particle swarm optimization
[28]		Hybrid particle swarm optimization
[29]		Ant colony optimization, pass enumerating
[30]	Quadratic programming	
[31]	Quadratic programming	Genetic algorithm
[32]	Dynamic programming	
[33]		Hybrid robust differential evolution
[34]		Genetic algorithm, artificial neural network
[35]		Genetic algorithm, simulated annealing, particle swarm optimization
[36]		Cuckoo optimization
[37]		Genetic algorithm, simulated annealing
[38]		Improved flower pollination
[39]		Pareto optimization, artificial neural network
[40]		Genetic programming
[41]		Iterative search, multi-objective genetic algorithm, genetic algorithm
[42]		Intelligent evolutionary algorithm
[43]		Genetic algorithm, cuckoo search, accelerated particle swarm
[44]		Analysis of variance
[45]		Bat algorithm, divide and conquer strategy
[46]	Special linearization method, linear mathematical programming	

Most optimization methods from the analyzed papers consider manufacturing cost maximization as the objective function. However, other papers use other optimization criteria, such as maximization of material removal rate, minimization of production time, minimization of surface roughness, and minimization of cutting temperature. Based on the current literature, it might be appreciated that the optimization mathematical models do not contain enough elements regarding the insurance of the machined-surface quality because they do not consider surface integrity. From this viewpoint, the depth of cut must be understood differently from the speed and feed rate. The depth of cut is directly connected to the surface integrity (Figure 1), and surface integrity is a very important concept used for appraising the machined-surface quality. The present paper develops a method focused on the concept of surface integrity for determining the depth of cut related to the routing sheet for machining front faces of cast iron work pieces.

## 2. Method Development

This section of the paper develops ideas from previous authors' research [8], approaching the determination of the technological sequences and the depths of cut for the front-face turning of cast iron parts. The considered basic criterion ensures the final surface integrity.

### 2.1. Mathematical Models

For determining the depths of cut for the current tool pass ( $d_{cf}$ ), the components of surface integrity from the previous pass must be eliminated (integrated into  $d_{cf}$  following Figure 1) to obtain new surface integrity (related to the current pass). This mechanism must work for all passes of the technological route. The technological route contains chained pairs of current and previous operations. Thus, the couple of current and previous operations represents an important link in process planning. Each previous operation becomes current for determining a new depth of cut. The concept of CPMP works in this manner. The mathematical models related to  $d_{cf}$  calculation are structures of relations in which the components of the surface integrity and other variables related to the geometrical errors of the surface to be machined and fixing errors are found. For establishing these mathematical models, certain data gathered by the authors from industrial practice, the searched literature [10,11], and also work in progress results obtained by the authors were considered. These data have been mathematically modeled by regression analysis (using software tools from the Department of Manufacturing Engineering). It was convenient to obtain information regarding the whole layer  $Rz_p + S_p$  (sum of previous surface roughness and spoiled superficial layer). From the industrial experience, it resulted that the values of certain parameters from these models depend on the geometric features of the part/billet, as well as on the casting process accuracy grade. The paper considers five casting process accuracy grades in accordance with the industrial practice and ISO 8062-1994 [47]. Grade 1 refers to the most accurate casting process, and grade 5 refers to the less accurate casting process. The casting process accuracy grade is considered by variable  $cab$ . The mathematical models for calculating the depths of cut regarding the three types of front-face turning are presented below.

#### 2.1.1. Calculation of the Depth of Cut for Rough Turning

The current operation is rough turning, and the previous operation refers to the cast billet.

$$\delta_{cib} = 2 \cdot c1 \cdot Dm^{b1} \cdot L^{b2} \cdot c2^{cab}, \quad (2)$$

$$Rz_{cib} + S_{cib} = c3 \cdot Dm \cdot cab + c4 \cdot Dm + c5 \cdot cab + c6, \quad (3)$$

$$\varepsilon F_{cib} = c20 \cdot D^{b10}, \quad D \in [10, 800], \quad (4)$$

$$\varepsilon Ca_{x_{rft}} = c21 \cdot Df^{b11} + c22 \cdot Df^{b11} \cdot cab, \quad (5)$$

$$d_{rft} \geq \delta_{cib} + Rz_{cib} + S_{cib} + \varepsilon F_{cib} + \varepsilon Ca_{x_{rft}}. \quad (6)$$

#### 2.1.2. Calculation of the Depth of Cut for Semi-Finishing Turning

The current operation is semi-finishing turning, and the previous operation is rough turning.

$$\delta_{rft} = 2 \cdot c11 \cdot L_{rft}^{b6}, \quad (7)$$

$$Rz_{rft} + S_{rft} = c12 \cdot cab^{b7}, \quad (8)$$

$$\varepsilon F_{rft} = c23 \cdot D^{b10}, \quad (9)$$

$$\varepsilon Ca_{x_{sft}} = c24 \cdot Df^{b12}, \quad (10)$$

$$d_{sft} \geq \delta_{rft} + Rz_{rft} + S_{rft} + \varepsilon F_{rft} + \varepsilon Ca_{x_{sft}}. \quad (11)$$

### 2.1.3. Calculation of the Depth of Cut for Finishing Turning

The current operation is finishing turning, and the previous operation is semi-finishing turning.

$$\delta_{sft} = 2 \cdot c16 \cdot L_{sft}^{b9}, \tag{12}$$

$$Rz_{sft} + S_{sft} = c17, \tag{13}$$

$$\epsilon F_{sft} = c25 \cdot D^{b10}, \tag{14}$$

$$\epsilon Cax_{fft} = c24 \cdot Df^{b12}, \tag{15}$$

$$d_{fft} \geq \delta_{sft} + Rz_{sft} + S_{sft} + \epsilon F_{sft} + \epsilon Cax_{fft}. \tag{16}$$

The coefficients and exponents from relations (2)–(16) are presented in Table 2 and were obtained by regression analysis in accordance with the above explanation.

**Table 2.** Coefficients and exponents from relations (2), . . . , (16).

c1	b1	b2	c2	c3	c4	c5	c6	c20	b10	c21	b11	c22
0.031	0.153	0.359	1.34	0.0000163	0.000131	0.044	0.357	0.0004	1.3723	0.0274	0.205	0.00432
c11	b6	c12	b7	c23	b10	c24	b12					
0.055	0.350	0.0174	1.79	0.000023	1.3723	0.0307	0.254					
c16	b9	c17	c25	b10	c24	b12						
0.023	0.342	0.05	0.000012	1.3723	0.0307	0.254						

### 2.2. CDFTCI Software Tool

The mathematical models (2)–(16) and the database (Table 2) have been integrated into the new software tool named CDFTCI (calculation of depth of cut for facing turning of cast iron), presented as the flow chart in Figure 2 and user interface in Figure 3.

Description of the module CDFTCI: After data input, the determination of the technological sequences for machining the considered front face follows. The decision variable is the roughness Ra. Then, for each technological sequence, calculated are the depths of cut ( $d_{cf}$ ), previous dimensions ( $L_{pre}$ ), standardized dimensions ( $L_{pren}$ ), and the real depths of cut ( $d_{cfreal}$ ). The results are stored in Table t(3,3). The coordinating parameter is surface integrity. After calculating a technological sequence, L1 and tft are updated, and the next technological sequence is calculated (if applicable). After closing the cycle controlled by counter p, the billet dimension ( $L_{cib}$ ) and the related tolerance ( $\delta_{Lcib}$ ) are determined. The results are summarized as sequences of multi-pass-facing turning (Table t1(3,4)). The user interface is presented in Figure 3. Description of user-computer interface: The user interface contains four areas. The first area is for data entering (left side) and contains fields for numerical data, buttons for choosing the surface position, the roughness, and the casting process grade. The next area, on the right side, presents a passive image of the part, used as an aid for specifying the mode in which the surface position is established (internal/external), as well as for Dn and Ln. The third area contains three buttons: OK, Part Image, and Close. The Part Image button is for re-displaying the passive image as many times as required. After data validation, the fourth area automatically appears instead of the second area and contains the obtained results.

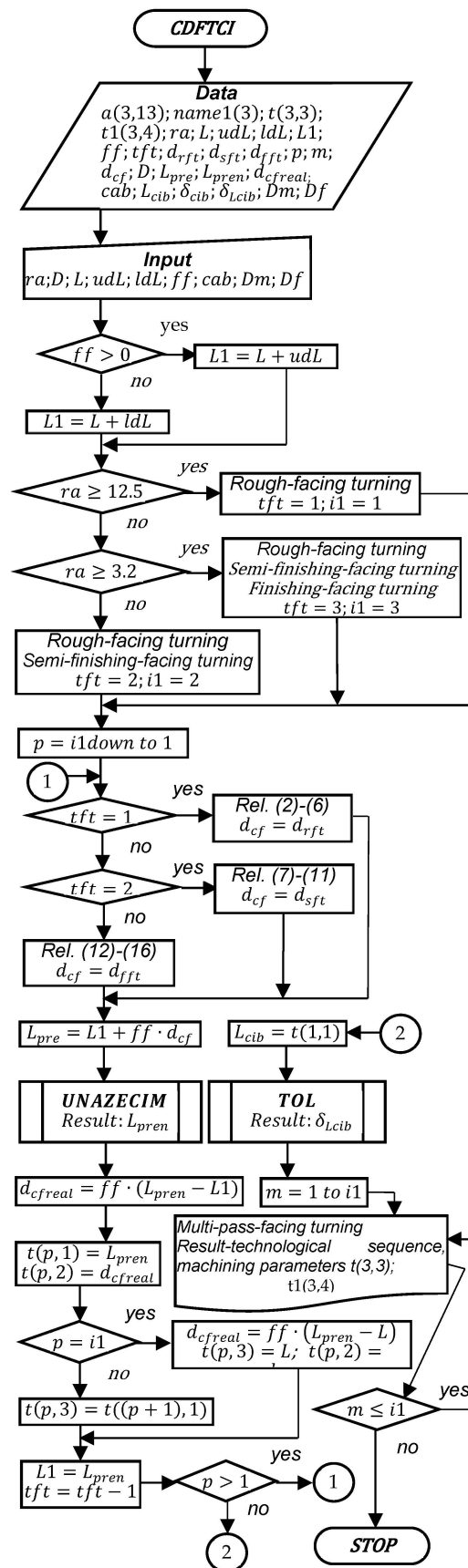


Figure 2. Flow chart of the CDFTCI module.

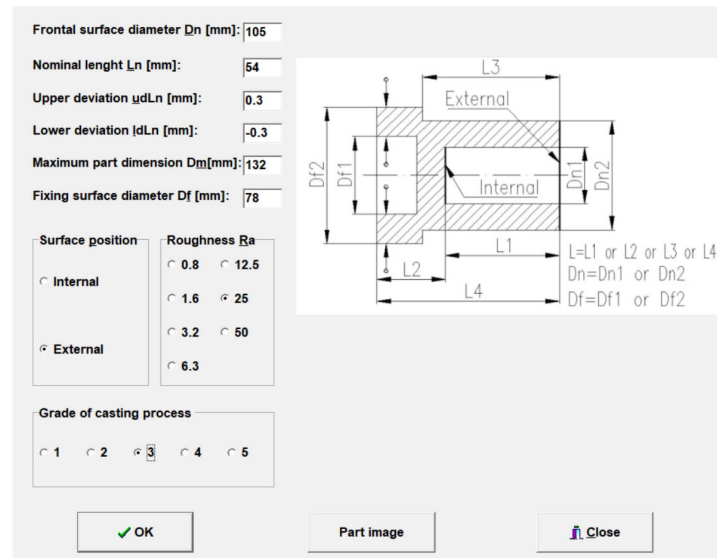


Figure 3. User interface.

### 3. Results of the Case Study

For the belt pulley from din Figure 4 (material EN-GJL-200 cast iron), the following elements are determined: a) the routing sheet and the depths of cut for turning of the front faces having the following dimensions: ●  $\phi 105$  with the roughness  $Ra = 25$  and  $L = 54$ ; ●●  $\phi 72^{+0.074}$  with the roughness  $Ra = 3.2$  and  $L = 54$  and b) the dimensional characteristics of the billet (including the tolerances). By running the software module CDFTCI, the technological sequences for machining the two mentioned front faces were obtained in accordance with Figures 5 and 6. These figures illustrate the obtained results, meaning the values of the depths of the cut, as well as the diameters of the two front faces after machining (the right sides of the figures). It is mentioned that for  $L = 54$ , the tolerances for the free dimensions have been adopted ( $\pm 0.3$ ). In the same manner, similar data have been obtained for the other front faces of the part (necessary for billet design). For determining the billet dimensions, there are also necessary data regarding the cylindrical surfaces of the part (the depths of cut). These data have been obtained using another software developed by the authors and presented in [8]. Thus, the billet shape from Figure 7 has been obtained.

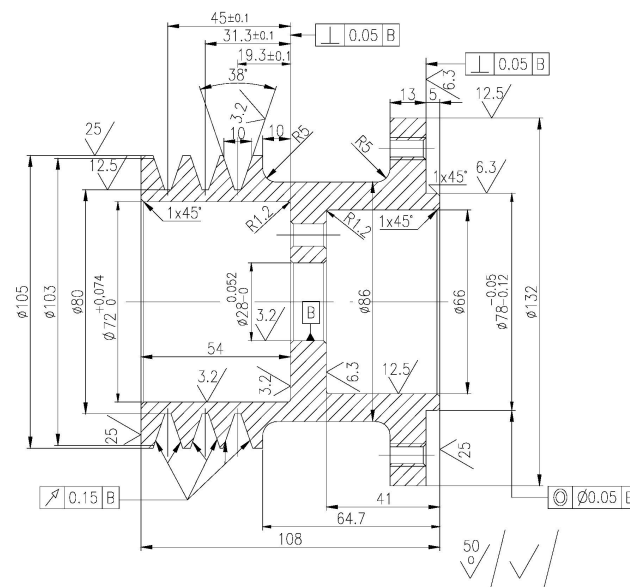


Figure 4. Analyzed part-belt pulley.

Frontal surface diameter Dn [mm]: 105  
 Nominal length Ln [mm]: 54  
 Upper deviation  $\mu dLn$  [mm]: 0.3  
 Lower deviation  $ldLn$  [mm]: -0.3  
 Maximum part dimension Dm[mm]: 132  
 Fixing surface diameter Df [mm]: 78

Surface position: Internal / External  
 Roughness Ra: 0.8, 1.6, 3.2, 6.3, 12.5, 25, 50

Grade of casting process: 1, 2, 3, 4, 5

**RESULTS**  
 Inputted Data:  
 Frontal surface diameter D [mm] =105  
 Nominal length Ln [mm] =54  
 Upper deviation  $\mu dLn$  [mm] =0.3  
 Lower deviation  $ldLn$  [mm] =-0.3  
 Maximal part dimension Dm [mm] =132  
 Fixing surface diameter Df [mm] =78  
 Roughness Ra [micr] =25  
 Surface position =1  
 Grade of casting process =3

Technological sequence for surface machining  
 Lme=54 Ra=25

Machining process	Prev. Dim.	Depth	Curr. Dim.
Rough FaciTurn	56.5	2.5	54

Length of the billet [mm]=56.5; Casting tolerance [mm]=1.8

Multi-pass turning	Depth	n	d1	d2
Rough FaciTurn	2.5	2	1	1.5

OK Part image Close

Figure 5. Results for facing turning  $\phi 105$ , L = 54, Ra = 25.

Frontal surface diameter Dn [mm]: 72  
 Nominal length Ln [mm]: 54  
 Upper deviation  $\mu dLn$  [mm]: 0.3  
 Lower deviation  $ldLn$  [mm]: -0.3  
 Maximum part dimension Dm[mm]: 132  
 Fixing surface diameter Df [mm]: 78

Surface position: Internal / External  
 Roughness Ra: 0.8, 1.6, 3.2, 6.3, 12.5, 25, 50

Grade of casting process: 1, 2, 3, 4, 5

**RESULTS**  
 Inputted Data:  
 Frontal surface diameter D [mm] =72  
 Nominal length Ln [mm] =54  
 Upper deviation  $\mu dLn$  [mm] =0.3  
 Lower deviation  $ldLn$  [mm] =-0.3  
 Maximal part dimension Dm [mm] =132  
 Fixing surface diameter Df [mm] =78  
 Roughness Ra [micr] =3.2  
 Surface position =1  
 Grade of casting process =3

Technological sequence for surface machining  
 Lme=54 Ra=3.2

Machining process	Prev. Dim.	Depth	Curr. Dim.
Rough FaciTurn	50.6	2.1	52.7
Semif. FaciTurn	52.7	0.7	53.4
Finish FaciTurn	53.4	0.6	54

Length of the billet [mm]=50.6; Casting tolerance [mm]=1.8

Multi-pass turning	Depth	n	d1	d2
Rough FaciTurn	2.1	2	0.9	1.2
Semif. FaciTurn	0.7	1	0.7	0
Finish FaciTurn	0.6	1	0.6	0

OK Part image Close

Figure 6. Results for facing turning  $\phi 72$ , L = 54, Ra = 3.2.

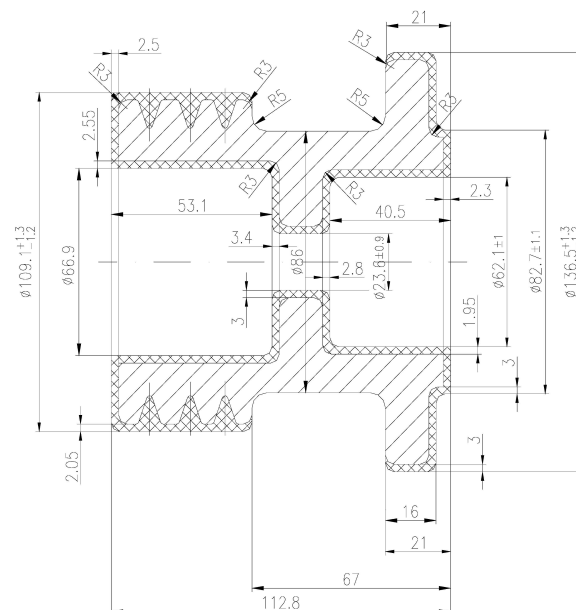


Figure 7. The billet corresponding to the analyzed part.

#### 4. Discussion

From the literature review (Section 1), it results that determining the depth of cut is done by machining parameters optimization, considering an economic criterion. The analyzed optimization mathematical models do not include the relationship between the depth of cut and the surface integrity. This aspect might lead to objective function optimization but does not guarantee to obtain the desired machined-surface quality. In the case of Figure 5, the dimension that must be obtained is  $\phi 105$  (external front face), having the roughness  $Ra = 25 \mu\text{m}$  and  $L = 54 \text{ mm}$ . CDFTCI software has determined the technological sequence—rough-facing turning with the total depth of cut = 2.5 mm divided into two passes ( $n = 2$ ). The first pass is made with a depth of cut of 1 mm, and the second one is made with a depth of cut of 1.5 mm. The total depth of cut is determined by considering the surface integrity in accordance with Formula (6). In the case of Figure 6, the dimension that must be obtained is  $\phi 72^{+0.074}$  (internal front face), having the roughness  $Ra = 3.2 \mu\text{m}$  and  $L = 54 \text{ mm}$ . CDFTCI software has determined three technological sequences with depths of cut of 2.1 mm, 0.7 mm, and 0.6 mm, respectively. Rough turning is made by two passes with the depths of cut of 0.9 mm and 1.2 mm, respectively. The depths of cut are also determined by considering the surfaces integrity, in accordance with Formulas (6), (11), and (16). We mention that all these calculations are made by the CDFTCI software tool. The division of the depth of cut into two passes helps the tool protection. The results supplied by the CDFTCI software tool are found on the billet drawing (Figure 7); thus:  $53.1 = 54 + 2.5 - 3.4$ . Final surface integrity is obtained by the process of successive transformations of the previous surface integrity into the current surface integrity, in accordance with Figure 1 and Formula (1). The industrial practice has confirmed the dependence of the components of surface integrity on the geometric features of the part and billet. This finding has allowed the determination of the mathematical models (2)–(16). The semi-finishing technological sequence might be excluded, but, in this case, the depths of cut for rough machining must increase.

#### 5. Conclusions

The present paper falls within process planning and machining process optimization. In this way, the approaches from the paper are aimed at the automatic establishment of routing sheets and a novel modality for calculating the depths of cut. The main conclusions are presented as follows:

- (a) The quality of the machined surface must not be reduced only to the surface roughness;
- (b) Surface integrity is a very important indicator for the assessment of the machined-surface quality, and it is directly related to the performance of a product;
- (c) The surface integrity influences the depth of cut. This means that the material layer having the thickness of the depth of cut must contain all the errors obtained in the surface and subsurface layers in the case of the previous machining operation. This fact is ensured by relations (2)–(16) conceived by the authors;
- (d) Determining the depth of cut requires knowledge of the routing sheet. For the routing sheet, the decisional element is the roughness of the surface to be machined;
- (e) After the routing sheet is known, the CDFTCI software tool calculates the depth of cut for every technological sequence. In this case, the decisional element is surface integrity;
- (f) The present paper leads to a novel approach to machining parameters optimization. First of all, the depths of cut must be calculated in accordance with ensuring the surfaces integrity. Then, the results obtained in this manner must be integrated into mathematical models for machining parameters optimization (into the objective function or/and as constraints);
- (g) The novelty of the present paper refers to the use of the surface integrity concept for establishing the routing sheet and the related depths of cut for turning the front faces of cast iron work pieces. In this way, the authors have developed a new/original software tool named CDFTCI (conceived in Delphi environment). This software is

- based on a small database associated with the original mathematical relations (2)–(16), whose role is to model the components of surface integrity and other errors;
- (h) The CDFTCI software also contributes to the calculation of the billets' dimensions regarding the front faces; with respect to the calculation of the billets' dimensions regarding the cylindrical surfaces, TESEQ and CDCIM software tools must be used [8];
  - (i) The CDFTCI software tool could be used as a standalone application, and it might be easily integrated into any CAP system and translated, if necessary, into other programming languages.

**Author Contributions:** All authors contributed to the elaboration of this paper. Conceptualization, C.G. and N.-V.I.; methodology, C.G. and N.-V.I.; software, N.-V.I. and G.O.; validation, C.G., N.-V.I. and G.O.; formal analysis, C.G. and N.-V.I.; investigation, C.G., N.-V.I. and G.O.; resources, C.G. and G.O.; data curation, C.G., N.-V.I. and G.O.; writing—original draft preparation, N.-V.I.; writing—review and editing, C.G., N.-V.I. and G.O.; visualization, C.G. and G.O.; supervision, N.-V.I. All authors have read and agreed to the published version of the manuscript.

**Funding:** This research received no external funding.

**Institutional Review Board Statement:** Not applicable.

**Informed Consent Statement:** Not applicable.

**Data Availability Statement:** Not applicable.

**Conflicts of Interest:** The authors declare no conflict of interest.

## Nomenclature

$d_{cf}, d_{cfreal}$	Calculated and real values of the depth of cut for facing turning (mm)
$\delta_{cib}, \delta_{rft}, \delta_{sft}$	Tolerances for: the billet, rough-facing turning, and semi-finish-facing turning, respectively (mm)
$D_m$	Maximum part dimension (mm)
$D(Dn), L(Ln)$	Work surface diameter and lengths (mm)
$Rz_{cib}, Rz_{rft}, Rz_{sft}$	Surface roughness for billet, rough-facing turning, and semi-finish-facing turning, respectively (mm)
$S_{cib}, S_{rft}, S_{sft}$	Subsurface layers spoiled for billet, rough-facing turning, and semi-finish-facing turning, respectively (mm)
$\varepsilon F_{cib}, \varepsilon F_{rft}, \varepsilon F_{sft}$	Flatness deviation for billet, rough-facing turning, and semi-finish-facing turning, respectively (mm)
$f_{sd}$	Specific flatness deviation ( $\mu\text{m}/\text{mm}$ )
$\varepsilon Ca_{x_{rft}}, \varepsilon Ca_{x_{sft}}, \varepsilon Ca_{x_{fft}}$	Axial clamping error regarding rough-facing turning, semi-finish-facing turning, and finish-facing turning, respectively (mm)
$a(3,13), name1(3)$	Matrices of the database
$ff$	Code variable: $ff = 1$ for external frontal surfaces and $ff = -1$ for internal frontal surfaces
$tft, i1$	Code variables regarding the number and types of technological sequences, respectively
$ra$	Required roughness ( $\mu\text{m}$ )
$udL(udLn), ldL(ldLn)$	Upper and lower deviations of L specified on the part drawing (mm)
$cab$	Casting process accuracy grade of the billet
$D_f$	Diameter of clamping surface (mm)
$d_{rft}, d_{sft}, d_{fft}$	Depths of cut for rough-facing turning, semi-finish-facing turning, and finish-facing turning, respectively (mm)
$p, m$	Counting parameters that control the running cycles of the CDFTCI module
$L_{pre}, L_{pren}$	Calculated and standardized values for the previous dimension regarding L (mm)
$L_{cib}, L_{rft}, L_{sft}$	The length of the part related to the front face for billet, rough-facing turning, and semi-finish-facing turning, respectively (mm)
$\delta_{Lcib}$	Final casting tolerance related $L_{cib}$ (mm)

$d_{tof}$ , $d_{cfi}$	Total depth of cut and depth of cut for a single pass related to facing turning, respectively (mm)
UNAZECIM	Subroutine that determines standardized value $L_{pren}$ regarding $L_{pre}$
TOL	Subroutine for determining the tolerance $\delta_{cib}$ (mm).

## References

1. Ulutan, D.; Ozel, T. Machining induced surface integrity in titanium and nickel alloys: A review. *Int. J. Mach. Tools Manuf.* **2011**, *51*, 250–280. [\[CrossRef\]](#)
2. Fang, F.; Gu, C.; Hao, R.; You, K.; Huang, S. Recent Progress in Surface Integrity Research and Development. *Engineering* **2018**, *4*, 754–758. [\[CrossRef\]](#)
3. Da Silva, R.B.; Sales, W.F.; Costa, E.S.; Ezugwu, E.O.; Bonney, J.; Da Silva, M.B.; Machado, A.R. Surface integrity and tool life when turning of Ti-6Al-4V with coolant applied by different methods. *Int. J. Adv. Manuf. Technol.* **2017**, *93*, 1893–1902. [\[CrossRef\]](#)
4. Xie, W.; Zhao, B.; Liu, E.; Chai, Y.; Wang, X.; Yang, L.; Li, G.; Wang, J. Surface integrity investigation into longitudinal-torsional ultrasonic vibration side milling for a TC18 titanium alloy-part I: The effects of cutting speed on cutting force and surface integrity. *Int. J. Adv. Manuf. Technol.* **2022**, *120*, 2701–2713. [\[CrossRef\]](#)
5. Pathade, H.P.; Gupta, M.K.; Kumar, N.; Pathade, M.P.; Wakchaure, P.B.; Gadhave, S.N.; Varpe, N.J.; Markad, A.V. A Review on Surface Integrity of Ball Burnishing Process. *Int. J. Res. Publ. Rev.* **2022**, *3*, 137–151. [\[CrossRef\]](#)
6. Malakizadi, A.; Bertolini, R.; Ducobu, F.; Kilic, Z.M.; Magnanini, M.C. Recent advances in modelling and simulation of surface integrity in machining—a review. *Procedia CIRP* **2021**, *15*, 232–240. [\[CrossRef\]](#)
7. Dumas, M.; Valiorgue, F.; Robaey, A.V.; Rech, J. Interaction between a roughing and finishing operation on the final surface integrity in turning. *Procedia CIRP* **2018**, *71*, 396–400. [\[CrossRef\]](#)
8. Ivan, N.V.; Gavrus, C.; Oancea, G. A new method for establishing the depths of cut for cast iron parts turning. *J. Braz. Soc. Mech. Sci. Eng.* **2018**, *40*, 496. [\[CrossRef\]](#)
9. Kovan, B.M. *Calculul Adașurilor de Prelucrare în Construcția de Mașini (Calculation of Tooling Allowances in Machine Building Industry)*; Mașghiz Publishing House: Moscow, Russia, 1953.
10. Kovan, B.M. *Technologie de la Construcția Mecanică (Machine Building Technology)*; Mir Publishing House: Moscow, Russia, 1970.
11. Picos, C.; Pruteanu, O.; Bohosievici, C.; Coman, G.; Braha, V.; Paraschiv, D.; Slătineanu, L.; Grănescu, T.; Marin, A.; Ionesii, V.; et al. *Proiectarea Tehnologiilor de Prelucrare Mecanică Prin Așchiere (Cutting Processes Technologies Planning)*; Editura Universitat Publishing House: Chișinău, Russia, 1992; Volumes 1 and 2.
12. Pratihari, D.K. Expert systems in manufacturing processes using soft computing. *Int. J. Adv. Manuf. Technol.* **2015**, *81*, 887–896. [\[CrossRef\]](#)
13. Zhu, L.; Jiang, Z.; Shi, J.; Jin, C. An overview of turn-milling technology. *Int. J. Adv. Manuf. Technol.* **2015**, *81*, 493–505. [\[CrossRef\]](#)
14. Baburaj, E.; Mohana Sundaram, K.M.; Senthil, P. Effect of high speed turning operation on surface roughness of hybrid metal matrix (Al-SiCp-fly ash) composite. *J. Mech. Sci. Technol.* **2016**, *30*, 89–95. [\[CrossRef\]](#)
15. Prasad, B.S.; Babu, M.P. Correlation between vibration amplitude and tool wear in turning: Numerical and experimental analysis. *Eng. Sci. Technol. Int. J.* **2017**, *20*, 197–211. [\[CrossRef\]](#)
16. Shin, Y.C.; Joo, Y.S. Optimization of machining conditions with practical constraints. *Int. J. Prod. Res.* **1992**, *30*, 2907–2919. [\[CrossRef\]](#)
17. Wang, J. Multiple-objective optimization of machining operations based on neural networks. *Int. J. Adv. Manuf. Technol.* **1993**, *8*, 235–243. [\[CrossRef\]](#)
18. Gupta, R.; Batra, J.L.; Lal, G.K. Determination of optimal subdivision of depth of cut in multipass turning with constraints. *Int. J. Prod. Res.* **1995**, *33*, 2555–2565. [\[CrossRef\]](#)
19. Chen, M.C.; Tsai, D.M. A simulated annealing approach for optimization of multi-pass turning operations. *Int. J. Prod. Res.* **1996**, *34*, 2803–2825. [\[CrossRef\]](#)
20. Onwubolu, G.C.; Kumalo, T. Optimization of multipass turning operations with genetic algorithms. *Int. J. Prod. Res.* **2001**, *39*, 3727–3745. [\[CrossRef\]](#)
21. Chen, M.C. Optimizing machining economics models of turning operations using the scatter search approach. *Int. J. Prod. Res.* **2004**, *42*, 2611–2625. [\[CrossRef\]](#)
22. Kumar, A.S.; Khan, M.A.; Thiraviam, R. Machining parameters optimization for alumina based ceramic cutting tools using genetic algorithm. *Mach. Sci. Technol.* **2006**, *10*, 471–489. [\[CrossRef\]](#)
23. Sardinas, R.Q.; Santana, M.R.; Brindis, E.A. Genetic algorithm-based multi-objective optimization of cutting parameters in turning processes. *Eng. Appl. Art. Intell.* **2006**, *19*, 127–133. [\[CrossRef\]](#)
24. Satishkumar, S.; Asokan, P.; Kumanan, S. Optimization of depth of cut in multi-pass turning using nontraditional optimization techniques. *Int. J. Adv. Manuf. Technol.* **2006**, *29*, 230–238. [\[CrossRef\]](#)
25. Wang, Y.C.; Chen, T. Modelling and optimization of machining conditions for the multi-pass dry turning process. *Proc. ImechE Part. B J. Eng. Manuf.* **2008**, *222*, 1387–1394. [\[CrossRef\]](#)
26. Srinivas, J.; Giri, R.; Yang, S.H. Optimization of multi-pass turning using particle swarm intelligence. *Int. J. Adv. Manuf. Technol.* **2009**, *40*, 56–66. [\[CrossRef\]](#)

27. Bharathi Raja, S.; Baskar, N. Optimization techniques for machining operations: A retrospective research based on various mathematical models. *Int. J. Adv. Manuf. Technol.* **2010**, *48*, 1075–1090. [[CrossRef](#)]
28. Costa, A.; Celano, G.; Fichera, S. Optimization of multi-pass turning economies through a hybrid particle swarm optimization technique. *Int. J. Adv. Manuf. Technol.* **2011**, *53*, 421–433. [[CrossRef](#)]
29. Xie, S.; Guo, Y. Optimisation of machining parameters in multi-pass turnings using ant colony optimisations. *Int. J. Mach. Mach. Mater.* **2012**, *11*, 204–220. [[CrossRef](#)]
30. Belloufi, A.; Assas, M.; Rezgoui, I. Optimization of Turning Operations by Using a Hybrid Genetic Algorithm with Sequential Quadratic Programming. *J. Appl. Res. Technol.* **2013**, *11*, 88–94. [[CrossRef](#)]
31. Lu, K.; Jing, M.; Zhang, X.; Liu, H. Optimization of sequential subdivision of depth of cut in turning operations using dynamic programming. *Int. J. Adv. Manuf. Technol.* **2013**, *68*, 1733–1744. [[CrossRef](#)]
32. Lu, K.; Jing, M.; Zhang, X.; Dong, G.; Liu, H. An effective optimization algorithm for multipass turning of flexible workpieces. *J. Intell. Manuf.* **2015**, *26*, 831–840. [[CrossRef](#)]
33. Yildiz, A.R. Hybrid Taguchi-differential evolution algorithm for optimization of multipass turning operations. *Appl. Soft Comput.* **2013**, *13*, 1433–1439. [[CrossRef](#)]
34. Mokhtari Homami, R.; Fadaei Tehrani, A.; Mirzadeh, H.; Movahedi, B.; Azimifar, F. Optimization of turning process using artificial intelligence technology. *Int. J. Adv. Manuf. Technol.* **2014**, *70*, 1205–1217. [[CrossRef](#)]
35. Gayatri, R.; Baskar, N. Performance analysis of non-traditional algorithmic parameters in machining operation. *Int J Adv Manuf Technol* **2015**, *77*, 443–460. [[CrossRef](#)]
36. Mellal, M.A.; Williams, E.J. Cuckoo optimization algorithm for unit production cost in multi-pass turning operations. *Int. J. Adv. Manuf. Technol.* **2015**, *76*, 647–656. [[CrossRef](#)]
37. Jabri, A.; Barcany, A.E.; Khalifi, A.E.I. Multipass Turning Operation Process Optimization Using Hybrid Genetic Simulated Annealing Algorithm. *Model. Simul. Eng.* **2017**, *2017*, 1940635. [[CrossRef](#)]
38. Xu, S.; Wang, Y.; Huang, F. Optimization of multi-pass turning parameters through an improved flower pollination algorithm. *Int. J. Adv. Manuf. Technol.* **2017**, *89*, 503–514. [[CrossRef](#)]
39. Abbas, A.T.; Pimenov, D.Y.; Erdakov, I.N.; Taha, M.A.; Soliman, M.S.; Rayes, M.M.E. ANN Surface Roughness Optimization of AZ61 Magnesium Alloy Finish Turning: Minimum Machining Times at Prime Machining Costs. *Materials* **2018**, *11*, 808. [[CrossRef](#)] [[PubMed](#)]
40. Abbas, A.T.; Benyahia, F.; Rayes, M.M.E.; Pruncu, C.; Taha, M.A.; Hegab, H. Towards Optimization of Machining Performance and Sustainability Aspects when Turning AISI 1045 Steel under Different Cooling and Lubrication Strategies. *Materials* **2019**, *12*, 3023. [[CrossRef](#)]
41. Radovanovic, M. Multi-objective optimization of multi-pass turning AISI 1064 steel. *Int. J. Adv. Manuf. Technol.* **2019**, *100*, 87–100. [[CrossRef](#)]
42. Mia, M.; Krolczyk, G.; Maruda, R.; Wojciechowski, S. Intelligent Optimization of Hard-Turning Parameters Using Evolutionary Algorithms for Smart Manufacturing. *Materials* **2019**, *12*, 879. [[CrossRef](#)]
43. Sofuoğlu, M.A.; Çakır, F.H.; Gürgeç, S. An efficient approach by adjusting bounds for heuristic optimization algorithms. *Soft Comput.* **2019**, *23*, 5199–5212. [[CrossRef](#)]
44. Danish, M.; Rubaice, S.; Ijaz, H. Predictive Modelling and Multi-Objective Optimization of Surface Integrity Parameters in Sustainable Machining Processes of Magnesium Alloy. *Materials* **2021**, *14*, 3547. [[CrossRef](#)] [[PubMed](#)]
45. Huang, X.; He, Z.; Chen, Y.; Xie, S. A Divide-and-Conquer Bat Algorithm with Direction of Mean Best Position for Optimization of Cutting Parameters in CNC Turnings. *Comput. Intell. Neurosci.* **2022**, *2022*, 4719266. [[CrossRef](#)] [[PubMed](#)]
46. Gavrus, C.; Ivan, N.V.; Oancea, G. Machining Parameters Optimization Based on Objective Function Linearization. *Mathematics* **2022**, *10*, 803. [[CrossRef](#)]
47. ISO 8062; International Standard ISO 8062. ISO: Geneva, Switzerland, 1994.

**Disclaimer/Publisher’s Note:** The statements, opinions and data contained in all publications are solely those of the individual author(s) and contributor(s) and not of MDPI and/or the editor(s). MDPI and/or the editor(s) disclaim responsibility for any injury to people or property resulting from any ideas, methods, instructions or products referred to in the content.